Colloidal Zeolites as Host Matrix for Copper Nanoclusters

J. Kecht,[†] Z. Tahri,[‡] V. De Waele,*[,‡] M. Mostafavi,[‡] S. Mintova,*[,†] and T. Bein[†]

Department of Chemistry and Biochemistry, University of Munich, Butenandtstrasse 11, 81377 Munich, Germany, and Laboratoire de Chimie Physique−ELYSE, Centre National de la Recherche Scientifique−University Paris Sud 11, 91405 Orsay, France

Received October 20, 2005. Revised Manuscript Received April 20, 2006

Nanosized zeolites stabilized in water suspensions are used as host matrix for the stabilization of copper clusters. The metal clusters are formed by γ radiolytic reduction of copper-containing large pore zeolites with FAU- (three-dimensional channels) and LTL- (one-dimensional channels) type structures in colloidal form. A selective stabilization of different metal species in the zeolite host matrix is demonstrated depending on the irradiation conditions, type of framework architecture, and copper content in the zeolite. The formation process of different species, that is, Cu^0 or/and Cu^I, within FAU and LTL zeolites was followed by UV−vis spectroscopy during the entire irradiation process. The transparency of the irradiated colloidal zeolite suspensions allows the absorption measurements to be carried out with low scattering from the zeolite particles having a size of about 50 nm. The use of nanosized crystals stabilized in water suspensions led to the formation of homogeneously distributed copper species all over the zeolite particles and not only on their surface.

Introduction

Supported copper nanoclusters inside the cages of molecular sieve hosts are expected to possess size-dependent electronic properties and nonlinear optical features.[1,2] On the other hand, the behavior of copper clusters in various standard reactions, such as click chemistry, cycloadditions, etc., is dependent on their size and degree of homogeneous distribution in the host matrix.[3,4] Moreover, the formation of copper (Cu^I) species during the reduction of zeolites containing Cu^{II} species is important for their catalytic activity and selectivity and mainly for the selective reduction of NO_x.[5−7]

Despite the intensive research in catalysis, the formation process of various metal clusters and emergence of different species during the reduction process of metal ions confined in porous zeolitic hosts is still not well understood. Zeolites are attractive host materials, as they have regular channel systems, providing crystallographic defined locations for reduced metal species. As a consequence, the size of the clusters inside the zeolites can be limited by the steric restrictions originating from their channels and cages, and at the same time their apertures can limit the amount of metal species diffusing from the zeolitic hosts. In some cases, the metal clusters inside the zeolite cages have been confined, and further agglomeration to bigger metal particles has been avoided, as is demonstrated in ref 8.

Recently, metal clusters of nearly uniform size have been generated by decarbonylation of metal carbonyl clusters with specific nuclearities inside the zeolite cages.[9] A similar approach for the preparation of clusters involves thermal decomposition of a precursor material, such as sodium azide or metal−organic compounds impregnated inside the zeolite channels.[10,11] Besides, easily volatile elements, for instance cadmium or alkali metals, have been introduced in host matrices by sorption of metal vapors.[12] More common approaches comprise the reduction of metal cations incorporated in zeolites by preliminary ion exchange, where as a reducing agent molecular hydrogen is used at elevated temperatures.[13] In the latter method, a migration of metal clusters leading to further agglomeration into large metal particles outside the zeolite crystals or in the bulk is sometimes observed.

Reduction of metals in aqueous solutions is also possible by addition of hydride anions or similar species.[14] However, two main problems have been arising when the latter approach is applied: (i) the reduction is not homogeneous due to the mixing of the two reactant solutions, leading to a wide distribution of metal cluster sizes in the solution, and

* Corresponding authors: e-mail svetlana.mintova@cup.uni-muenchen.de (S.M.) or vincent.dewaele@lcp.u-psud.fr (V.D.W.).
[†] University of Munich.
[‡] CNRS−University Paris Sud.

(1) Magruder, R. H.; Haglund, R. F., Jr.; Yang, L.; Wittig, J. E.; Zuhr, R. A. *J. Appl. Phys.* **1994**, *76*, 708.
(2) Celep, G.; Cottancin, E.; Lerme, J.; Pellarin, M.; Arnaud, L.; Huntzinger, J. R.; Vialle, J. L.; Broyer, M.; Palpant, B.; Boisron, O.; Melinon, P. *Phys. Rev. B: Condens. Matter Mater. Phys.* **2004**, *70*, 165409.
(3) Thathagar, M. B.; Beckers, J.; Rothenberg, G. *Adv. Synth. Catal.* **2003**, *345*, 979.
(4) Pachon, L. D.; van Maarseveen, J. H.; Rothenberg, G. *Adv. Synth. Catal.* **2005**, *347*, 811.
(5) Kieger, S.; Delahay, G.; Coq, B.; Neveu, B. *J. Catal.* **1999**, *183*, 267.
(6) Torre-Abreu, C.; Henriques, C.; Ribeiro, F. R.; Delahay, G.; Ribeiro, M. F. *Catal. Today* **1999**, *54*, 407.
(7) Coq, B.; Delahay, G.; Durand, R.; Berthomieu, D.; Ayala-Villagomez, E. *J. Phys. Chem. B* **2004**, *108*, 11062.
(8) Gates, B. C. *Chem. Rev.* **1995**, *95*, 511.
(9) Guzman, J.; Gates, B. C. *Dalton Trans.* **2003**, *17*, 3303.
(10) Ozin, G. A.; Gil, C. *Chem. Rev.* **1989**, *89*, 1749.
(11) Doskocil, E. J.; Mankidy, P. J. *Appl. Catal., A* **2003**, *252*, 119.
(12) Goldbach, A.; Barker, P. D.; Anderson, P. A.; Edwards, P. P. *Chem. Phys. Lett.* **1998**, *292*, 137.
(13) Watzky, M. A.; Finke, R. G. *J. Am. Chem. Soc.* **1997**, *119*, 10382.
(14) Linnert, T.; Mulvaney, P.; Henglein, A.; Weller, H. *J. Am. Chem. Soc.* **1990**, *112*, 4657.

10.1021/cm052312c CCC: $33.50
Published on Web 06/06/2006

(ii) the reduction of metal cations (Ni^{2+}, Co^{3+}, Cu^{2+}, etc.) is not completed due to the low strength of the chemical reducing agents.

Radiolysis is a powerful process for the preparation of metal or metal oxide particles in various solutions.[15−17] Mainly γ radiolysis has been used to reduce metal ions in hydrated and dehydrated micro- and mesoporous compounds in powder form.[18−21] However, significant changes in the framework topology and subsequent damage of the porous hosts induced by the creation of radicals during the irradiation were observed.

In this paper we report a new strategy for the preparation of copper clusters in metal-containing suspensions of zeolite nanocrystals by γ radiolysis. This method has the advantage of being relatively gentle, that is, the reduction is carried out at ambient conditions, allowing precise control of the irradiation setting and thus providing quantitative information for the entire dynamic process of metal reduction. Furthermore, when the irradiation is carried out in colloidal suspensions, the samples contain large amounts of water, and therefore the γ rays interact with the water and thus result in well-defined radiolytic products. In addition, as the reducing radicals are produced in water, it is possible to achieve a complete reduction of metals incorporated in the zeolite nanocrystals without any radiation damage of the zeolite matrix. Finally, the transparent zeolite suspensions are also well adapted for UV−vis absorption measurements,[22,23] and hence it is possible to follow in situ the formation of metallic clusters in the FAU[24] and LTL[24] zeolite hosts.

Experimental Section

Synthesis of Nanosized FAU- and LTL-type Zeolites. Zeolite Y nanocrystals with FAU-type structure were prepared from a clear precursor solution with the molar composition $2.37(TMA)_2O{:}0.05Na_2O{:}1Al_2O_3{:}4.16SiO_2{:}244H_2O$. After aging of the solutions at room temperature (RT) without agitation for 3 days, hydrothermal (HT) treatment at 100 °C for 72 h was carried out (for details see ref 25). Zeolite L with LTL-type structure was synthesized from a precursor solution free of organic additives having the chemical composition $5K_2O{:}0.2Na_2O{:}0.5Al_2O_3{:}10SiO_2{:}200H_2O$. The crystallization was carried out at 170 °C for 2 h in a microwave oven (details can be found in ref 26). After the complete crystallization of both colloidal solutions, the resulting zeolite crystals were recovered by multistep centrifugation and washed with doubly distilled (dd) water.

Table 1. Elemental Ratios for Zeolites Y and L

sample	Cu/Al[a]	Na/Al[a]	K/Al[a]	TMA/Al[b]
CuY-1	0.348	0.124		0.179
CuY-2	0.115	0.360		0.280
CuL-1	0.178		0.700	
CuL-2	0.091		0.873	

[a] Based on ICP-AES measurements. [b] Based on thermogravimetric analysis.

Ion Exchange of Nanosized FAU- and LTL-type Zeolites. Zeolites Y (FAU) and L (LTL) were stabilized in water suspensions at pH = 9 and a concentration of solid particles of about 1.5 wt %. The colloidal suspensions were subjected to ion exchange without preliminary calcination of the FAU zeolite. Several samples were prepared with different copper loadings by mixing copper nitrate (0.1 M) with zeolite suspensions, giving solutions containing 6 mmol of Cu^{2+}/g of zeolite (samples CuY-1 and CuL-1), 0.6 mmol of Cu^{2+}/g of zeolite (sample CuY-2), and 0.3 mmol of Cu^{2+}/g of zeolite (sample CuL-2). The ion-exchange process was carried out at 60 °C for 16 h, and then the solutions were purified by two-step centrifugation and redispersed in doubly distilled water. The chemical composition of all samples after ion exchange is summarized in Table 1.

γ Irradiation of Cu-FAU and Cu-LTL Suspensions. The colloidal suspensions containing zeolite Y and L nanoparticles were diluted with deionized water (18 MΩ directly before irradiation); the metal concentration was chosen to be in the range 10^{-3}−10^{-5} mol/L for expedient detection of the metals by absorption spectroscopy. After the dilution, 0.2 M 2-propanol was added to the zeolite suspensions, to convert the oxidizing OH radicals generated by the radiolysis of water into reducing alcohol radicals. The high sensibility of the copper clusters leading to fast oxidation was overcome by deaeration under N_2 atmosphere immediately before irradiation in a Pyrex cell; the latter was connected with an optical cell that allows recording of the spectra under N_2 atmosphere. The optical cell of Suprasil was protected by lead shielding during the entire process of γ-irradiation. The irradiation source was a ^{60}Co panoramic γ-facility of 3000 Ci with a maximum dose rate of 4 kGy·h^{-1}. All samples reported here are irradiated with a dose rate of 1000 Gy·h^{-1}. The absorption spectra for samples CuY-1 and CuY-2 are measured between 0 and 8 kGy in different steps.

Characterization. The crystalline structure of samples before and after ion exchange was determined by X-ray diffraction (XRD) measurements performed on a Stoe powder diffractometer in transmission geometry (Cu Kα, λ = 1.5406 Å). The size of the crystalline domains in the zeolite samples was determined on the basis of the Scherrer equation, by use of the line broadening of several Bragg reflections (the fitting of the diffraction patterns was carried out with WinXPOW Size/Strain1.02, STOE & Cie GmbH). Prior to the size determination, the instrumental peak broadening was resolved by measuring lanthanum hexaboride as a reference material (Aldrich). In addition, dynamic light

(15) Belloni, J.; Mostafavi, M. *Metal Clusters Chem.* **1999**, *2*, 1213.
(16) Belloni, J.; Mostafavi, M. *Stud. Phys. Theor. Chem.* **2001**, *87*, 411.
(17) Henglein, A. *Ber. Bunsen-Ges.* **1995**, *99*, 903.
(18) Gachard, E.; Belloni, J.; Subramanian, M. A. *J. Mater. Chem.* **1996**, *6*, 867.
(19) Michalik, J.; Van der Pol, A.; Reijerse, E. J.; Wasowicz, T.; De Boer, E. *Appl. Magn. Reson.* **1992**, *3*, 19.
(20) Vijayalakshmi, R.; Kapoor, S.; Kulshreshtha, S. K. *Solid State Sci.* **2002**, *4*, 489.
(21) Hornebecq, V.; Antonietti, M.; Cardinal, T.; Treguer-Delapierre, M. *Chem. Mater.* **2003**, *15*, 1993.
(22) Mintova, S.; De Waele, V.; Hoelzl, M.; Schmidhammer, U.; Mihailova, B.; Riedle, E.; Bein, T. *J. Phys. Chem. A* **2004**, *108*, 10640.
(23) Mintova, S.; De Waele, V.; Schmidhammer, U.; Riedle, E.; Bein, T. *Angew. Chem., Int. Ed.* **2003**, *42*, 1611.
(24) Baerlocher, Ch.; Meier, W. M.; Olson, D. H. *Atlas of Zeolite Framework Types*; Elsevier: Amsterdam, 2001; pp 132, 170.
(25) Mintova, S.; Olson, N. H.; Bein, T. *Angew. Chem., Int. Ed.* **1999**, *38*, 3201.
(26) Hölzl, M.; Mintova, S.; Bein, T. *Stud. Surf. Sci. Catal.* **2005**, *158A*, 11.

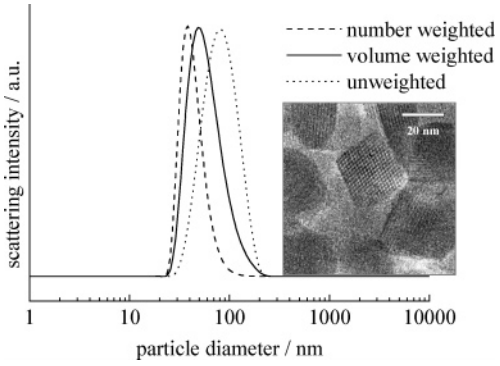

Figure 1. Particle size distribution curves for zeolite Y. The inset shows a TEM micrograph of the corresponding sample.

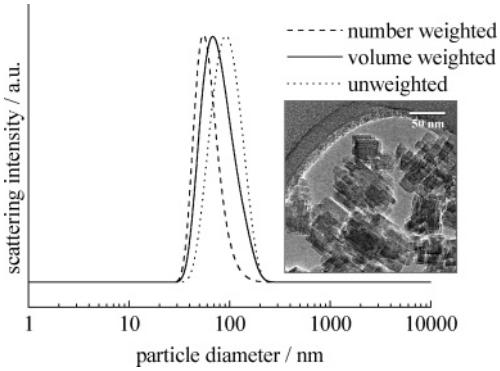

Figure 2. Particle size distribution curves for zeolite L. The inset shows a TEM micrograph of the corresponding sample.

scattering (DLS) measurements in colloidal suspensions were performed with a Malvern Zetasizer-Nano instrument equipped with a 4 mW He−Ne laser (633 nm) and avalanche photodiode detector. The chemical composition of the zeolite samples before and after ion exchange was determined by inductively coupled plasma atomic emission spectroscopy (ICP-AES; Varian−Vista). Thermogravimetric analyses (TGA) of dried zeolite samples were performed to determine the amount of organic template still present in zeolite Y samples (Netzsch STA 440 C TG/DSC, heating rate of 10 K/min in a stream of synthetic air ∼25 mL/min).

UV−vis spectra of colloidal suspensions after radiolysis were recorded on a Hewlett-Packard HP8453 spectrometer. Transmission electron microscopic (TEM) images were taken on irradiated zeolite samples, to confirm the formation of metal clusters and determine their size by use of a JEOL JEM 2011 microscope operating at 200 kV. The irradiated samples were prepared in a glovebox under nitrogen atmosphere, followed by drying in a vacuum for 2 h prior to TEM study.

Results and Discussion

Nanosized FAU- and LTL-type Zeolite Suspensions. The FAU-type framework structure consists of a three-dimensional channel system with large pore openings of 7.4 Å defined by the aperture of 12-membered rings, while LTL-type zeolite consists of a one-dimensional channel system running along the crystallographic *c*-axis defined by 12-membered rings with a free diameter of 7.1 Å.[24] The colloidal zeolite nanocrystals with FAU-type structure were stabilized in aqueous suspensions with a constant concentration and pH. The particle size distribution curves of colloidal suspensions were recorded by DLS in a backscattering geometry, revealing a monomodal particle size distribution prior to the ion-exchange treatment. The hydrodynamic diameter of FAU crystals varied from 20 to 100 nm, when the light scattering intensity is expressed as unweighted particle size distribution dependence (Figure 1). However, the apparent mean particle diameter decreased significantly by about 30−50 nm when the distribution was number- or volume-weighted (see Figure 1). The high crystallinity of the zeolite samples was confirmed by X-ray patterns collected from the purified and dried samples prior to the postsynthesis treatment. Only Bragg reflections representing the FAU crystals without any impurities or other phases were observed (patterns are not shown). The mean crystalline domain size of the dried FAU particles was determined on the basis of the Scherrer equation, giving a mean diameter of the crystalline domains of about 80 nm, which is in good agreement with the DLS measurements. In addition, the high crystallinity and the typical morphological appearance of FAU particles are demonstrated with the TEM picture shown as inset in Figure 1. The crystalline fringes of pure FAU zeolite are well-resolved. The template-free aluminosilicate solutions subjected to microwave heating result in the crystallization of LTL-type zeolite. The particle size, degree of polydispersity, and colloidal stability were determined by DLS. A monomodal particle size distribution is observed for the LTL samples, giving rise to a peak centered at 50 nm, when the scattering intensity is expressed as number-weighted dependence (Figure 2). The peak is right-shifted to 80−100 nm for LTL zeolites when the light scattering intensity is weighted by volume (Figure 2). However, a smaller crystalline domain size of about 37 nm is calculated from the Scherrer equation, which is significantly smaller than the size determined by DLS. This can be explained by the morphology of the LTL particles. In the case of DLS, the size of the particles is calculated on the basis of the scattering of light from agglomerates consisting of smaller nanosized LTL crystallites. The TEM image of LTL crystals (Figure 2) prior to ion exchange reveals that the LTL sample consists of crystalline nanosized domains (20−40 nm) that are well aligned and form the ultimate aggregates with a final size of 80−100 nm.

The stabilized water suspensions of LTL and FAU zeolites were subjected to ion exchange with copper according to the procedure described above. The chemical compositions of the zeolites before and after ion exchange were determined by ICP-AES, and the results are summarized in Table 1. As can be seen, the potassium in the LTL zeolite (Si/Al = 2.85) was not completely exchanged for copper due to the high affinity of K for the zeolite framework. The copper content is about 35% and 18% of the cation-exchange capacity for samples CuL-1 and CuL-2, respectively. However, an overexchange degree has been observed for LTL zeolite, which is likely caused by additional anionic species such as OH^- partially counterbalancing the positive charge of copper cations. Similar data for hydroxide species in zeolites after ion exchange with transition metals have been reported elsewhere.[27,28]

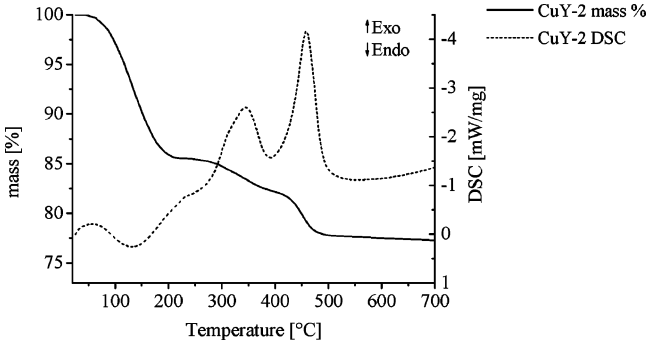

Figure 3. TG and DSC curves of sample CuY-2.

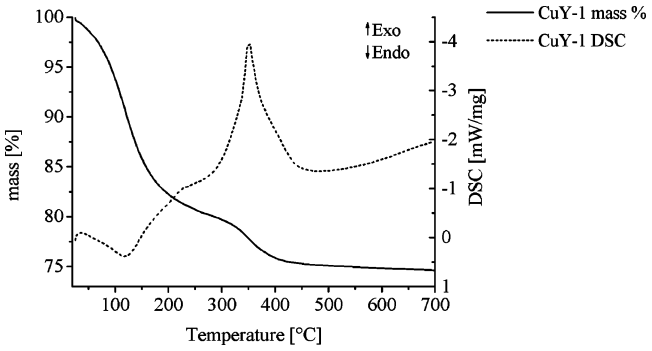

Figure 4. TG and DSC curves of sample CuY-1.

In the case of FAU zeolite (Si/Al = 1.70), the ion exchange of Na^+ and TMA^+ for Cu^{2+} is not complete either (Table 1). The residual sodium ions in the zeolite are probably due to the slow exchange kinetics of the S1 and S1′ sites in the FAU structure, as has been reported previously.[29] The bulky tetramethylammonium cation used as a template for the synthesis of zeolite Y probably is exchangeable only if it is located in the zeolite supercage; it cannot be removed completely from the β cages. We note that all FAU samples were subjected to ion exchange without preliminary drying and calcination, and therefore a large amount of TMA^+ is present in the crystals. The copper content is about 70% and 23% in samples CuY-1 and CuY-2, respectively (see Table 1). The quantity of TMA in the zeolite samples was determined by heating the same amount of powder (10 mg) in a TG crucible, which allows a quantitative comparison of the samples. Figures 3 and 4 show the TG/DSC curves of samples CuY-2 and CuY-1, respectively. The zeolitic water is removed from the two samples below 200 °C, while the organic additive (TMA) is combusted between 300 and 470 °C. The total amount of water is about 20 and 14 wt % for samples CuY-1 and CuY-2, respectively. These results illustrate the increased affinity of molecular sieves with high Cu loading toward water. On the other hand, the amount of TMA was decreased with progressive ion exchange, and about 8 and 5 wt % TMA was decomposed in samples CuY-2 and CuY-1, respectively. The DSC curves suggest the presence of two locations of TMA in the FAU structure from which the template is combusted at 320 and 460 °C. We attribute these two exothermic effects to TMA molecules located in the β cages and supercages of FAU zeolite, respectively, which are removed from the structure at different temperatures.

In the case of sample CuY-1, the total sum of copper, sodium, and TMA content is giving 100%, indicating that the copper is not coordinated by additional ions such as hydroxide. However, in sample CuY-2, the sum of Na, TMA, and Cu content is 87%, and the remaining 13% presumably is due to the presence of protons. This observation is in agreement with the removal of TMA cations from the supercages, under repeated washing of FAU zeolite before and after the ion-exchange treatment.

γ Radiolysis of Cu-FAU Suspensions. All zeolite nanoparticles containing different amounts of Cu were stored in H_2O suspensions and thus subjected to γ-radiolysis in a Pyrex cell. The redox chemistry of copper is governed by the following one-electron semiequations associated with one-electron reduction potentials:

$$Cu^+ + e^- \leftrightarrows Cu^0_{metal} \; (E = 0.56V_{NHE}) \tag{1}$$

$$Cu^{2+} + e^- \leftrightarrows Cu^+ \; (E = 0.16V_{NHE}) \tag{2}$$

$$Cu^+ + e^- \leftrightarrows Cu^0 \; (E = -2.7V_{NHE}) \tag{3}$$

In this notation, the index metal is used to indicate that the atom belongs to a metal particle and in that way has been distinguished from free atoms. The difference between the redox potentials corresponding to the metal copper and copper atoms according to eqs 1 and 3, respectively, should be noticed. A variation of the ratio $E°$ (Cu_n^+/Cu_n) is expected, since the atomic potential for $E°$ (Cu^+/Cu^0) is $-2.7V_{NHE}$,[30] while for $E°$ (Cu_7^+/Cu_7) it is $-0.4V_{NHE}$,[31] and the bulk electrode potential is $0.52V_{NHE}$ (NHE = normal hydrogen electrode). It is well-known that the reduction potentials of copper clusters and oligomers vary from −2.7 to 0.56 V, depending on their size and environment. Hence, in the earliest stage of the cluster formation, eqs 2 and 3 can be combined and reaction 4 will be favored:

$$Cu^{2+} + Cu^0 \rightarrow 2Cu^+ \tag{4}$$

As the clusters are growing in size, their redox potential increases as well, and the disproportionation reaction is expected to dominate:

$$Cu^+ + Cu^+ \rightarrow Cu^{2+} + Cu^0_{metal} \tag{5}$$

Under the conditions used here, the reduction of copper can proceed by the reaction of two reducing species produced by radiolysis in the water−alcohol solutions, that is, the solvated electron (e^-_{solv}) and the alcohol radicals $\bullet C(CH_3)_2OH$, according to the redox equations:

(27) Bae, D.; Seff, K. *Microporous Mesoporous Mater.* **1999**, *33*, 265.
(28) Bae, D.; Seff, K. *Microporous Mesoporous Mater.* **2000**, *40*, 219.
(29) Weidenthaler, C.; Mao, Y.; Schmidt, W. Impact of Zeolites and Other Porous Materials on the New Technologies at the Beginning of the New Millennium. *Stud. Surf. Sci. Catal.* **2002**, *142B*, 1857.
(30) Henglein, A. *Ber. Bunsen-Ges.* **1977**, *81*, 556.
(31) Khatouri, J.; Mostafavi, M.; Amblard, J.; Belloni, J. *Chem. Phys. Lett.* **1992**, *191*, 351.

$$(CH_3)_2CO + e^- + H^+ \leftrightarrow \bullet(CH_3)_2COH\ (E = -1.8V_{NHE}) \quad (6)$$

$$nH_2O + e^- \leftrightarrow e^-_{solv}\ (E = -2.9V_{NHE}) \quad (7)$$

The solvated electrons formed by water radiolysis are therefore able to reduce Cu^{2+} into Cu^0 according to the following reactions, and the corresponding rate constants in bulk solutions are given below:[32]

$$Cu^{2+} + e_{solv}^- \rightarrow Cu^+\ (k = 2.7 \times 10^{10}\ L\cdot mol^{-1}\cdot s^{-1}) \quad (8)$$

$$Cu^+ + e_{solv}^- \rightarrow Cu^0\ (k = 3.3 \times 10^{10}\ L\cdot mol^{-1}\cdot s^{-1}) \quad (9)$$

On the other hand, the radical of alcohol can only reduce Cu^{II} to Cu^{I}, but it is not strong enough to form copper atoms. The radiolytic yields representing the formation of e^-_{solv} and $\bullet C(CH_3)_2OH$ species in water, expressed as G in micromoles per gray, are well defined due to the experimental conditions, and they are $G(e^-_{solv}) = 0.26\ \mu M/Gy$ and $G(\bullet C(CH_3)_2OH) = 0.32\ \mu M/Gy$, correspondingly. In the zeolite suspensions, the reducing species are formed in the bulk water that surrounds the nanosized zeolite crystals and diffuse in the three-dimensional zeolite framework structures, leading to reduction of Cu^{II} to Cu^{I} and Cu^0 species.

The UV−vis absorption spectra of samples CuY-2 and CuY-1 recorded at several irradiation doses are depicted in Figures 5 and 6, correspondingly. In both samples, the concentration of zeolite particles was kept identical and only the amount of copper cations (Cu^{2+}) in the zeolite particle introduced by ion exchange is different (see Experimental Section). By comparison of these absorption spectra, it is apparent that the reactivity of copper in both samples involves different species of copper. Sample CuY-2 shows a large absorption band located between 270 and 600 nm, with a maximum at 480 nm, which is formed in the beginning of the irradiation process (0.3 kGy). A possible assignment of that is the appearance of charge-transfer bands of O−Cu−O and Cu−O−Cu complexes, which are expected to absorb in the regions of 320−370 and 400−440 nm, respectively.[33] In the same way, the generation of Cu-oxo species with a possible formula $[Cu-O-Cu]^{2+}$ located in the supercages of zeolite Y has been predicted for the selective catalytic reduction of NO_x.[34] However, it is obvious that all these species are reduced forms of Cu^{II}.

At higher irradiation doses, the evolution of the absorption spectra of sample CuY-2 is dominated by a large band structured in the near UV with a pronounced maximum in the range of 460−490 nm. This band is observed at irradiation doses between 0.6 and 3.6 kGy and is gradually shifted to higher wavelengths (see Figure 5). This band is located outside the range characteristic for the absorption of small metal copper oligomers or nanoclusters; however, Cu_2O particles can absorb in this region as well.[35] The same

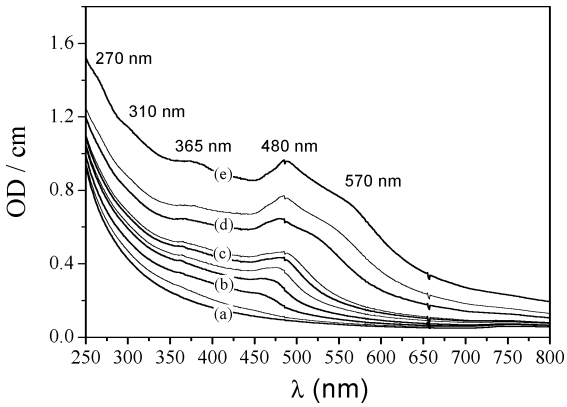

Figure 5. Absorption spectra of sample CuY-2 ($[Cu^{2+}] = 0.3 \times 10^{-3}$ M) before (a) and after irradiation with doses of (b) 0.6, (c) 1.5, (d) 2.7, and (e) 8.0 kGy.

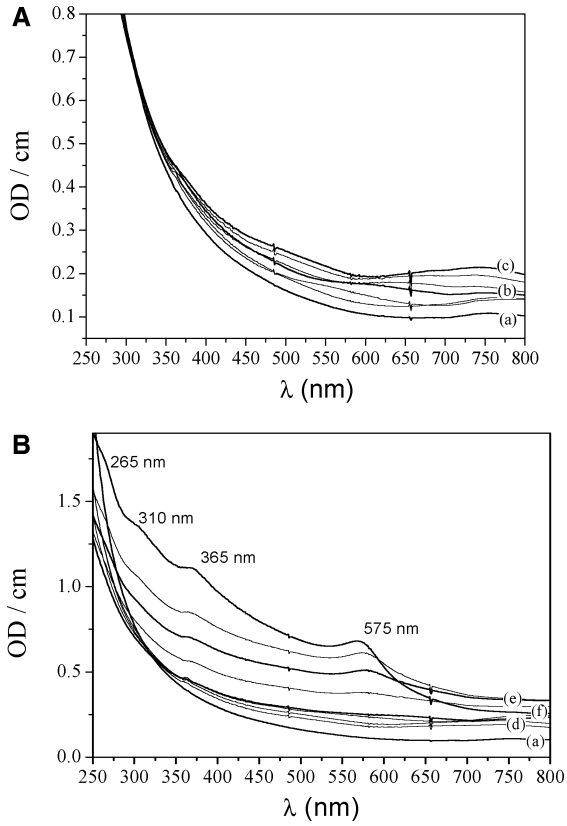

Figure 6. Absorption spectra of sample CuY-1 ($[Cu^{2+}] = 10^{-3}$ M) before (a) and after irradiation with doses of (b) 0.9, (c) 1.8, (d) 3, (e) 5.5, and (f) 8 kGy.

band at 480 nm has also been assigned to Cu^{I} species formed in poly(acrylic acid) systems.[36] Moreover, the absorption around 480 nm was ascribed to the presence of Cu^{I} species stabilized by CO_2^- molecules.[37] Similar to the results reported before, the appearance of the absorption band at 480 nm in sample CuY-2 is due to the presence of stabilized Cu^{I} cations in the FAU zeolite matrix. In this case, the Cu^{I} species become very stable since they are trapped in the zeolite framework. Assuming an extinction coefficient ϵ for the stabilized Cu^{I} species $\epsilon = 2000\ M^{-1}\ cm^{-1}$, as reported in

(32) Buxton, G. V.; Greenstock, C. L.; Helman, W. P.; Ross, A. B. *J. Phys. Chem. Ref. Data* **1988**, *17*, 513.
(33) Pestryakov, A. N.; Petranovskii, V. P.; Kryazhov, A.; Ozhereliev, O.; Pfander, N.; Knop-Gericke, A. *Chem. Phys. Lett.* **2004**, *385*, 173.
(34) Komatsu, T.; Nunokawa, M.; Moon, I. S.; Takahara, T.; Namba, S.; Yashima, T. *J. Catal.* **1994**, *148*, 427.
(35) Yang, M.; Zhu, J.-J. *J. Cryst. Growth* **2003**, *256*, 134.
(36) Ershov, B. G.; Janata, E.; Michaelis, M.; Henglein, A. *J. Phys. Chem.* **1991**, *95*, 8996.
(37) Anbar, M.; Bambenek, M.; Ross, A. B. *Selected specific rates of reactions of transients from water in aqueous solution. I. Hydrated electron*; Stanford Research Institute: Menlo Park, CA, 1973; p 54.

the literature, the amount of Cu^{I} can be calculated on the basis of the absorption spectra. The concentration of stabilized cations will be about 0.25×10^{-3} M, recorded for sample CuY-2 at the irradiation dose of 1.8 kGy. This number corresponds to the reduction of about 75% of the total amount of Cu^{2+} existing in sample CuY-2. The radiolytic yield of formation of Cu^{I} species $G(Cu^{I})$ is equal to 0.12 $\mu M \cdot Gy^{-1}$. In this case, the value for G is lower than the maximum radiolytic reduction yield based on the formation of solvated electrons and alcohol radicals. However, this value is in agreement with other results reported on the radiolytic yield $G(Cu)$, which is lower than the one measured for metals such as Pt, Ir, and Ag.[38]

The zeolite samples already containing Cu^{I} species were subjected to continuous irradiation, and the evolution of the absorption spectra has been followed. A broad shoulder at ~570 nm accompanied by an increase of the spectral features below 450 nm suggests the formation of copper clusters at higher irradiation doses above 2.7 kGy (see Figure 5, traces d and e). The band at 570 nm is a typical plasmon resonance corresponding to copper nanoclusters. The intensity of the band at 570 nm increases during the irradiation while its width is decreasing (see Figure 5). In addition to the formation of the plasmon absorption band, several others centered at ~265, ~310, and ~365 nm are observed in the spectra of sample CuY-2. These bands are related to the presence of oligomeric species Cu_2^{+}, which are in agreement with a previously made assignment for copper clusters synthesized in the presence of poly(acrylic acid); the bands at 292, 350, and 455 nm have been assigned to oligomers constituted of few atoms.[36] The metal clusters are formed via the reduction of Cu^{I} by the solvated electrons, and subsequent aggregation of the copper atoms results in the formation of Cu_2^{+} species. Moreover, the consecutive reduction and aggregation/coalescence processes create even bigger clusters. The species Cu_2^{+} are regarded as precursors for the formation of copper cluster, when the irradiation is carried out in aqueous solutions (see eq 10).[39] Neutral and cationic clusters are generated by further agglomeration of different atomic or oligomeric species according to the following formula:

$$Cu^{0} + Cu^{+} \rightarrow Cu_2^{+} \quad (10)$$

$$Cu_x^{a+} + Cu_y^{b+} \rightarrow Cu_{x+y}^{(a+b)+} \quad (11)$$

Furthermore, the formation of Cu_2^{+} can also proceed by the interactions between Cu^{+} cations stabilized by the alcohol radicals according to the following mechanism:[37,40,41]

$$(Cu(CH_3)_2\dot{C}OH)^{+} + Cu^{+} \rightarrow Cu_2^{+} + (CH_3)_2CO + H^{+} \quad (12)$$

The band at 365 nm could be related with Cu_2^{+} molecular species, as has been also specified in ref 39.

The spectra of sample CuY-1 have significantly different features, as depicted in Figure 6. The bands at ~310 and ~365 nm assigned to the copper oligomers are also present here. However, no absorption band at ~480 nm is observed. Instead, a development and a strong shift of two bands in the range of 400−800 nm is seen at irradiation doses up to 3.0 kGy. Moreover, at higher irradiation doses, the absorption at wavelengths greater than 600 nm is diminished again. The development of the copper cluster plasmon band at ~580 nm is clearly visible in sample CuY-1, and a shift to lower wavelengths at 575 nm under high irradiation doses (>8 kGy) is observed as well. Such evolution of the absorption plasmon band is typical for the growth of metallic nanoclusters. In the earliest stages, the plasmon band is broad, which is associated with the formation of subnanometric metallic clusters. As the aggregation process progresses, the width of the band decreases and its maximum is shifted toward shorter wavelengths. Another indication for the formation of copper clusters is provided by the observed change in the color of the zeolite suspensions; that is, at the end of the irradiation process, the color of the solution became a transparent red.

The correlation between the disappearance of the absorption band above 600 nm and the emergence of the cluster's plasmon band suggests that the species absorbing above 600 nm are the precursors for the metallic copper formed in the zeolite suspensions (Figure 6). The data for sample CuY-1 (in contrast to sample CuY-2) suggest that the formation of metallic copper does not proceed via stabilization of Cu^{I}. Since all the other conditions for preparation of samples CuY-1 and CuY-2 were identical, this particular behavior reflects the strong influence of the ion-exchange degree on the reactivity of Cu^{2+} in FAU-type molecular sieve.

γ Radiolysis of Cu-LTL Suspensions. Colloidal suspensions containing large-pore LTL zeolite with different copper loadings (CuL-1 and CuL-2) were subjected to γ radiolysis at conditions similar to those used for FAU samples. The spectra of samples CuL-1 and CuL-2 are shown in Figure 7. As can be seen, for both samples having low (CuL-2 ~ 0.08×10^{-3} M) and high (CuL-1 ~ 0.14×10^{-3} M) copper content, the formation process of metal copper clusters proceeds through formation of Cu^{I} species. After irradiation of sample CuL-2 with a dose of 250 Gy, about 80% of the Cu^{2+} cations were reduced to Cu^{I} species. The spectrum of CuL-2 is dominated by the absorption band at 480 nm (see Figure 7B). Under the same irradiation conditions, the spectrum of sample CuL-2 contains two bands at 480 and 570 nm, which are assigned to Cu^{I} and Cu^{0} nanoparticles, respectively. This is evidence that all Cu^{2+} ions have first been reduced to Cu^{I} species, and then a reduction of Cu^{I} into Cu^{0} takes place. In contrast to the FAU zeolite, it was not possible to stabilized directly copper metal oligomers in the LTL host without forming first the Cu^{I} species. The metal loading in the LTL zeolite is lower than in the FAU samples due to the lower ion-exchange capacity. Therefore, the formation process of metal clusters observed in the LTL zeolite is in agreement with the results obtained for FAU samples; that is, at lower metal content the formation of Cu^{I} species is favored.

(38) Kumar, M. *Radiat. Phys. Chem.* **2002**, *64*, 99.
(39) Buxton, G. V.; Green, J. C. *J. Chem. Soc., Faraday Trans. 1* **1978**, *74*, 697.
(40) Freiberg, M.; Mulac, W. A.; Schmidt, K. H.; Meyerstein, D. *J. Chem. Soc., Faraday Trans. 1* **1980**, *76*, 1838.
(41) Texier, I.; Mostafavi, M. *Radiat. Phys. Chem.* **1997**, *49*, 459.

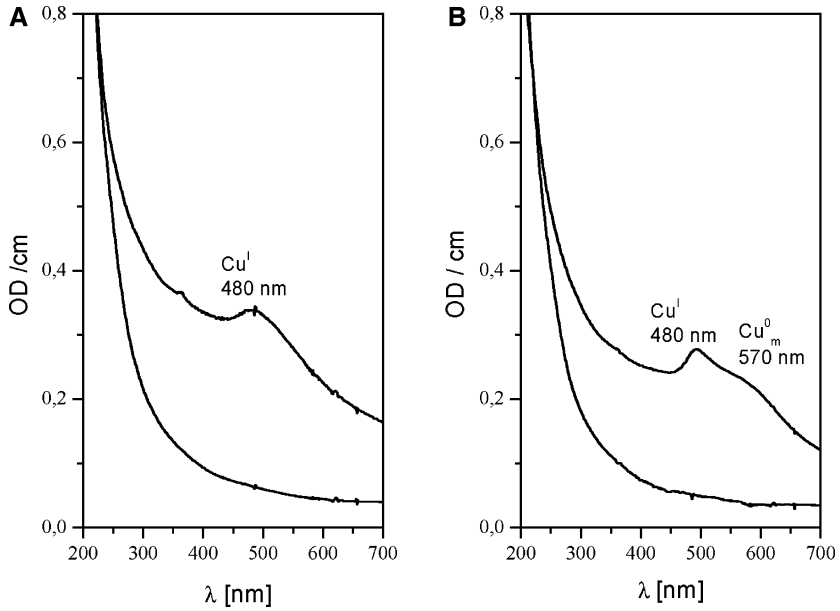

Figure 7. Absorption spectra of sample CuL-1 ($[Cu^{2+}] = 0.14 \times 10^{-3}$ M) (A) and CuL-2 ($[Cu^{2+}] = 0.08 \times 10^{-3}$ M) (B) before and after irradiation at a dose of 0.25 kGy.

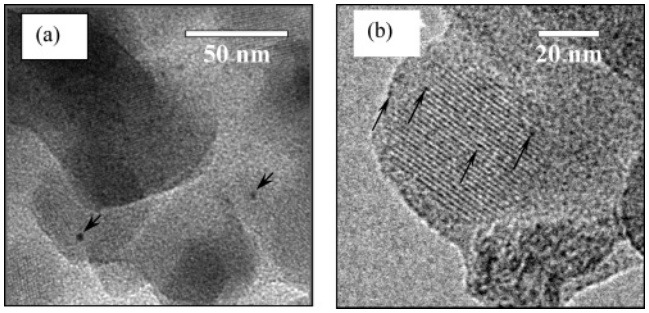

Figure 8. TEM images of sample CuY-1 after irradiation with a dose of 5.5 kGy. The arrows mark the position of copper particles.

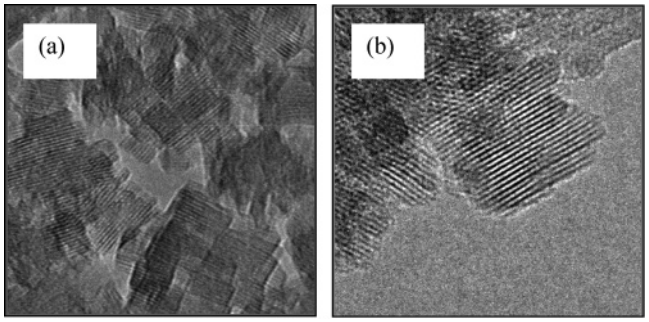

Figure 9. TEM image of sample CuL-1 before (a) and after (b) irradiation with a dose of 0.4 kGy. M = 20 nm.

The comparison of samples Y and L demonstrates that the type of the zeolite host materials and metal loading plays a significant role regarding the stabilization of various metal species. Time-resolved measurements are in progress to clarify and explain the different behavior of copper species located in these two zeolite hosts.

The emergence of the copper plasmon band in both colloidal suspensions CuY-1 and -2 and CuL-1 and -2 shows the generation of small copper clusters instead of large agglomerates or metallic precipitates that are often seen in nonstabilized copper solutions. However, it is not clear yet if these copper particles are located inside the zeolite framework or if they are firmly stabilized at the particle's surface. This point is of special interest considering their stability and possible migration of copper from zeolite hosts with big apertures.

As a complementary method for the characterization of copper clusters in the crystalline host materials, high-resolution transmission electron microscopy (HRTEM) was applied. The HRTEM images collected from sample CuY-1 treated at irradiation dose of 5.5 kGy reveal the formation of copper clusters (~2 nm) associated with the zeolite nanocrystals (Figure 8 a), as well as dark spots associated with small copper clusters located in the zeolite hosts can be distinguished. The FAU zeolite particles are slightly changed under prolonged exposure to the beam, since the originally sharp crystal edges appear rounded or in some cases amorphous material can be detected (Figure 8b). It is known that the colloidal zeolite nanoparticles can be easily amorphized, and for a short time the metallic clusters several angstroms in size, such as Au, Ag, Cu, etc., can be imaged. In the case of zeolite L, the one-dimensional channel system is almost completely occupied by copper species that follow the zeolite channels (see Figure 9).

The TEM data demonstrate the absence of agglomerates of copper metal clusters at the periphery of the individual zeolite crystallites. This finding suggests a fairly homogeneous distribution of copper species in the zeolite host crystals. Under the beam, the one-dimensional channel system of zeolite L is almost completely destroyed; however, the black-colored wires are still there. This observation is in good agreement with the UV−vis spectra, where the formation of copper clusters and their alignment as wires within the zeolite channels is proven.

Conclusions

A new approach for creation of copper clusters confined in nanosized zeolite particles based on γ radiolytic reduction in water suspensions has been reported. The current approach

permits the preparation of different types of copper clusters under gentle conditions and allows selective stabilization of diverse species in the zeolite hosts depending on the irradiation conditions, as well as on the copper content of zeolites. The formation process of Cu^0 or Cu^I species selectively stabilized in the zeolite hosts with different framework architectures were followed by UV−vis spectroscopy in the transparent zeolite suspensions.

The use of nanosized crystals stabilized in water suspensions led to a fairly homogeneous distribution of the reduced copper species over the entire zeolite particles and not on their surfaces. The approach reported here is promising for the preparation of metal-containing zeolites, for instance, for applications in catalysis or antimicrobial compounds, where the metal species should be homogeneously distributed all over the zeolite host matrix. Moreover, this method can be transferred to many other metal cations, owing to the strong reducing potential of the radicals formed by radiolysis.

Acknowledgment. We gratefully acknowledge funding from the BFHZ and DFG-CNRS, and Dr. M. Döblinger for the TEM images.

CM052312C